Pergamon

Int. J. Solids Structures Vol. 35, Nos 31–32, pp. 4121–4132, 1998
© 1998 Elsevier Science Ltd
All rights reserved. Printed in Great Britain
0020–7683/98 $19.00 + .00

PII: S0020–7683(97)00305–3

IMPLICATIONS OF THE SIZE EFFECT METHOD FOR ANALYZING THE FRACTURE OF CONCRETE

RAVINDRA GETTU,* HÉCTOR SALDÍVAR,
Universitat Politecnica de Catalunya, ETSECCPB, Edificio C1, Jordi Girona 1–3, E-08034 Barcelona, Spain

and

MOHAMMAD TAGHI KAZEMI
Sharif University of Technology, Tehran, Iran

(*Received* 9 *October* 1996; *in revised form* 25 *February* 1997)

Abstract—The size effect method (SEM) of Bažant is reviewed and its range of applicability is examined through comparisons with data from tests on notched and unnotched beams of normal and high strength concrete. Its behavior and scope are discussed with respect to some other models, including the multifractal scaling model. The SEM reflects the effect of brittleness on the failure adequately. Moreover, the model is able to satisfactorily predict the failure loads of fracture specimens, as long as the initial cracks are not very small compared to the maximum aggregate size and the specimen dimensions. For other cases, the predictions are over-conservative. © 1998 Elsevier Science Ltd. All rights reserved.

INTRODUCTION

The size effect model (SEM) proposed by Bažant in 1984, and extended in later works, has led to a framework for simulating the failure of concrete and other quasi-brittle materials, as well as a simple experimental method for characterizing their fracture parameters. The SEM is a nonlinear fracture mechanics model in the sense that it is based on two independent material parameters derived from modifications of linear elastic fracture mechanics (LEFM) , which is characterized by a single fracture parameter. The second parameter is necessary to account for the effect of the fracture process zone of concrete, which is the zone at the crack-tip where energy is dissipated during fracture. Furthermore, the model utilizes an effective LEFM crack whose length is the sum of the traction-free crack and an effective length of the fracture process zone (Bažant and Kazemi, 1990). Consequently, the SEM is often classified as an effective crack model (Elices and Planas, 1993).

As its name suggests, the SEM is founded on the size-dependence of the failure loads. This phenomenon can be introduced through the LEFM stress intensity factor, which is proportional to the applied load, and is a function of the geometry and size of the specimen or structure:

$$K_I = \frac{P}{b\sqrt{d}}\sqrt{g(\alpha)} \tag{1}$$

where P = applied load, b = specimen thickness, d = the characteristic specimen dimension, $\alpha = a/d$, a = crack or notch length and $g(\alpha)$ is the geometry-dependent non-dimensional energy release rate. In LEFM, crack propagation occurs when $K_I = K_{Ic}$, where K_{Ic} is a material property known as the critical stress intensity factor or fracture toughness. As a

*Author to whom correspondence should be addressed. Tel.: 34 93 401 7354. Fax: 34 93 401 1036. E-mail: gettu@etseccpb.upc.es.

consequence, there is a size effect, which can be demonstrated by considering geometrically-similar notched specimens that fail without significant crack propagation, that is, at the initial value of α, say, $\alpha = \alpha_0$. If the nominal stress at failure is defined as $\sigma_N = P_u/bd$, where P_u is the failure load, the LEFM size effect is obtained from eqn (1) as:

$$\sigma_N = K_{Ic} \frac{1}{\sqrt{g(\alpha_0)}} \frac{1}{\sqrt{d}} \tag{2}$$

where the failure stress is inversely proportional to the square root of the specimen size (d), for the constant K_{Ic} and $g(\alpha_0)$, that is, for the same material and specimen geometry. At the other extreme, failure that is insensitive to the stress intensity is governed by size-independent stresses, as in plastic materials.

The present work reviews the SEM, and discusses the range of applicability of the model in the characterization and prediction of size effects in fracture specimens. The fracture parameters are determined using specimens cut from the halves of previously-tested larger size specimens to avoid the need for three sets of moulds and to decrease the quantity of material used. Two concretes with different strengths and brittleness have been utilized in the experimental study. The comparison of the results with those of the multifractal scaling model is also presented.

REVIEW OF THE SIZE EFFECT MODEL

The size effect observed in different sizes of geometrically-similar concrete specimens does not always follow the trend of LEFM discussed earlier. In most cases, the size effect becomes weaker than that of LEFM, with a gradual decrease in the brittleness of the failure mode, as the specimen size decreases. On the basis of such a transition exhibited in the failure mode of notched concrete specimens, Bažant (1984) proposed the following relation between the nominal failure stress (σ_N) and the characteristic dimension (d) for geometrically similar specimens, which is known as the size effect law or size effect model (SEM):

$$\sigma_N = \frac{B}{\sqrt{1+\beta}}; \quad \beta = \frac{d}{d_0} \tag{3}$$

where B and d_0 are empirical parameters (that depend on the structural geometry and the material characteristics), and β is called the brittleness number (Bažant and Pfeiffer, 1987). Generally, higher values of B and d_0 indicate higher strength and lower brittleness, respectively. In some papers, Bf_t is used instead of B, where f_t is a reference strength (for example, tensile strength) that is introduced to make B non-dimensional. However, this has led some researchers to incorrectly conclude that the application of the model needs the determination of the tensile strength and that the parameters obtained depend on this value. It is, therefore, suggested here that B be used instead, with units of stress, to avoid confusion. Similarly, the parameter d_0 is preferred to $\lambda_0 d_a$ that was used in early papers, which has led some to assume (Carpinteri *et al.*, 1995), again incorrectly, that the trend given by SEM depends only on the aggregate size (since d_a was defined as the maximum aggregate size and λ_0 was the empirical parameter). The maximum nominal stress also needs some clarification. It has often been defined as $\sigma_N = c_n P_u/bd$, where P_u is the peak load, b is the thickness, d is the reference dimension (say, beam depth), and c_n is a constant that is introduced for convenience in order to obtain a meaningful quantity, for example, the maximum tensile stress in a beam (Bažant and Kazemi, 1990). In the present work, c_n is omitted for simplicity. Note that none of the above-mentioned simplifications modify either the significance or the applicability of the model.

The asymptotes of eqn (3) are the failure criteria of size-independent strength (or limit stress; i.e., $\sigma_N = B$ for small d) and LEFM [i.e., $\sigma_N \propto d^{-1/2}$ for large d; as in eqn (2)]. Assuming that the former indicates ductile or plasticity-type failure and that the latter

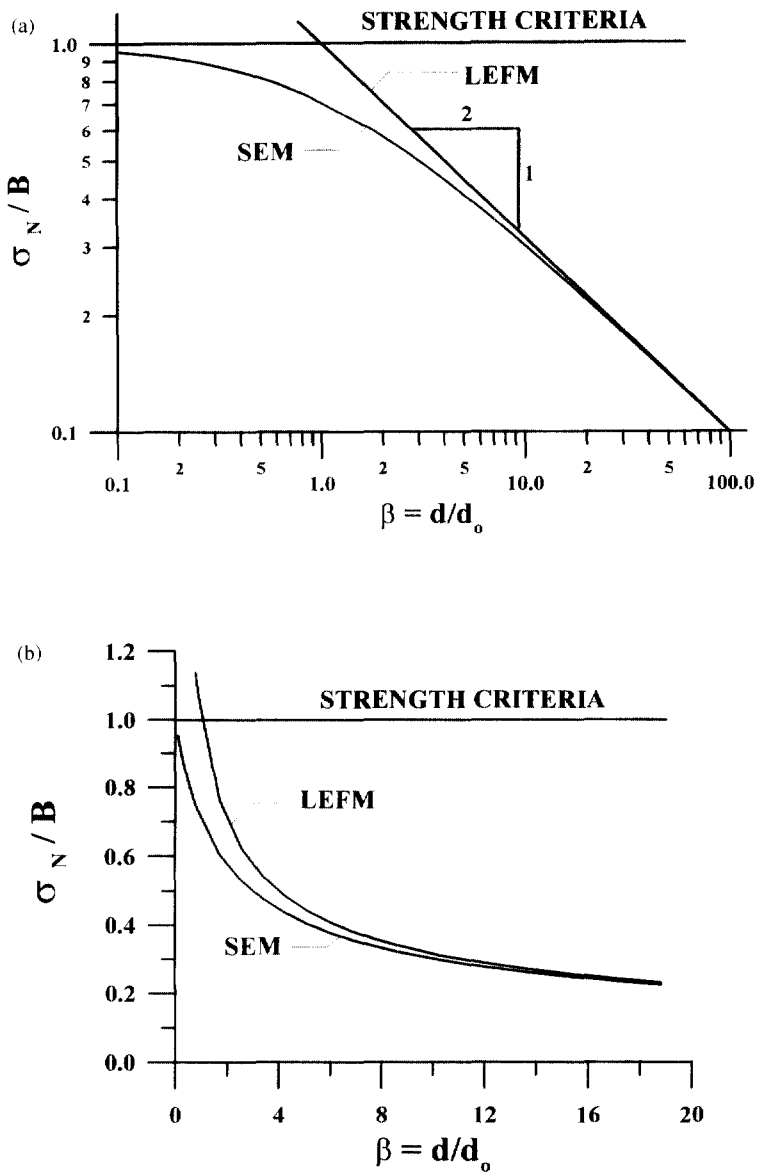

Fig. 1. The size effect model shown in (a) logarithmic and (b) linear plots.

represents ideal-brittle failure, the SEM demonstrates the tendency of the failure mode of geometrically similar structures to change gradually from ductile to brittle as their size increases. This trend is usually shown in a log–log plot, as in Fig. 1a. However, this diagram presented over a scale range of 1 : 1000, has often been misunderstood (Tang *et al.*, 1992; Carpinteri *et al.*, 1995) to imply that the strength approaches zero for real-size structures. When the SEM is presented in a linear plot, over a more practical range of $0.2 < \beta < 20$, as in Fig. 1b, it is obvious that the trend is similar to those observed in experiments. The failure stress reduces at a decreasing rate as the size increases but does not reach zero within the normal ranges of structures utilized and tested. Note that in both plots the trends corresponding to LEFM are obtained using eqn (2), with $K_{Ic} = B\{d_0 g(\alpha_0)\}^{1/2}$ (as defined by Bažant and Kazemi, 1990).

The most important application of the SEM is in material characterization. The transition in failure mode was used by Bažant to derive fracture parameters based on the extrapolation of the data from laboratory specimens to the LEFM asymptote of the SEM. As seen earlier, this limit, at which the parameters are defined, corresponds to very large

specimen size (or theoretically, to infinite size where geometry and size effects are absent). The parameters are (Bažant and Kazemi, 1990; Bažant *et al.*, 1991):

$$K_{Ic} = B\sqrt{d_0 g(\alpha_0)}; \quad G_f = \frac{K_{Ic}^2}{E}; \quad c_f = \frac{g(\alpha_0)}{g'(\alpha_0)} d_0; \quad \delta_c = \frac{8K_{Ic}}{E}\sqrt{\frac{c_f}{2\pi}} \tag{4}$$

where K_{Ic} = fracture toughness, G_f = fracture energy, E = modulus of elasticity, c_f = effective length of the fracture process zone, and δ_c = effective critical crack-tip opening displacement. The constants $g(\alpha_0)$ and $g'(\alpha_0)$ are the values of the non-dimensional energy release rate and its derivative at the relative initial crack length α_0 (= initial crack or notch length/beam depth). These LEFM functions, which depend on the specimen/structure geometry, have been determined for some cases (Bažant and Kazemi, 1990; RILEM, 1990) and can be obtained for others using elastic finite element analysis. A simple procedure for the experimental determination of the fracture parameters (used later in this study), known as the size effect method, has been specified in RILEM Draft Recommendation FMC2 (1990), using geometrically similar specimens of three different sizes. In order to avoid the effects of data scatter, the minimum size range of 1 : 4 and the use of three test specimens in each size are recommended.

The implications of the material characterization in terms of the SEM are important for purposes of materials engineering and structural design. In the former, K_{Ic} and c_f can be utilized as measures of the resistance against cracking and the pseudo-ductility of the material, respectively, in the process of developing better materials (cf Gettu and Shah, 1994). In structural design, the extension of the SEM to failures governed by concrete cracking has been studied and seems promising (cf Bažant *et al.*, 1994). The SEM has also been used as the basis for the definition of the brittleness of structural failure. Considering the brittleness number given in eqn (3) in terms of the parameters of eqn (4), we have

$$\beta = \frac{1}{c_f} \times \frac{g(\alpha_0)}{g'(\alpha_0)} \times d \tag{5}$$

which can be explained as:

[structural brittleness at failure] = [material brittleness] × [effect of structure geometry] × [size]

demonstrating that in addition to the material brittleness, the geometry and size of a structure influence its brittleness.

The SEM has been validated by Bažant *et al.* for several cases of failure, including those of notched specimens and structural elements (cf Bažant and Kazemi, 1990; Bažant *et al.*, 1994). From a study of these and other works, it can be stated that eqn (3) is clearly applicable to the cases of geometric similarity including the initial cracks or notches. In other words, eqn (3) describes the size effect on the failure of structures whose dimensions and initial crack lengths are scaled. On the other hand, the formulation of eqn (3) in terms of the parameters defined in eqn (4) leads to a more general form (Bažant and Kazemi, 1990):

$$\sigma_N = \frac{K_{Ic}}{\sqrt{g'(\alpha_0)c_f + g(\alpha_0)d}} \tag{6}$$

that extends the SEM to non-similar structures. More importantly, this makes it possible to predict the failure load of any specimen or structural geometry, not just specimens that are geometrically similar to the ones used to calibrate the model. It should, however, be noted that the SEM is directly applicable only to positive geometries (i.e., for $g'(\alpha_0) > 0$), where there is no propagation of the traction-free crack before failure. This aspect has been

discussed by Planas and Elices (1990b) who have shown that in non-positive geometries, the traction-free crack length at failure is not the same as the initial crack or notch length (i.e., $\alpha > \alpha_0$), and therefore, the failure load may be independent of the initial geometry, on which the SEM is based.

COMPARISON WITH OTHER NONLINEAR FRACTURE MECHANICS MODELS

Planas and Elices have studied the theoretical and experimental aspects of various nonlinear fracture models in detail, and explained their limitations and the equivalences between them. Their studies have included the SEM, the Two Parameter Fracture Model (TPFM) of Jenq and Shah (1985) and the Fictitious Crack Model of Hillerborg (1983). They demonstrated that all these models converge to LEFM behaviour for very large sizes and that their predictions are indistinguishable in the practical size range (Planas and Elices, 1990a; Elices and Planas, 1991; Elices *et al.*, 1996). However, the experimental calibration of these models varies significantly. As mentioned earlier, the parameters of the SEM are defined for a specimen of infinite size and are, therefore, theoretically size- and geometry-independent. However, the influence of the specimen size range used in their determination has not been studied thoroughly. On the other hand, the parameters of the TPFM may depend on the size and geometry of the specimen used in their determination (Elices and Planas, 1991; Mihashi *et al.*, 1996) necessitating a standard specimen for its experimental calibration. This is also the case of the fictitious crack model, which ideally needs a direct tension test for determining its parameters.

For practical purposes, the parameters of the SEM and TPFM can be considered as equivalent. That is, using the parameters of the TPFM, namely the fracture toughness (K_{Ic}^s) and critical crack-tip opening displacement ($CTOD_c$) as K_{Ic} and δ_c, respectively, in the SEM [see eqns (4) and (5)] the same values of failure loads in normal-size notched beams are obtained. This equivalence has also been proposed by other researchers (e.g., Bažant *et al.*, 1991; Gettu *et al.*, 1995; Karihaloo, 1995), and is illustrated in Fig. 2, where the predictions of the two models for three-point bend specimens (span/depth ratio = 4) of different depths and with a notch length $a_0 = 10$ mm are given for a cement mortar with $K_{Ic} = K_{Ic}^s = 0.955$ MPa-m$^{0.5}$, $\delta_c = CTOD_c = 0.00965$ mm and $E = 32.48$ GPa. The predictions are similar, especially for smaller specimens.

One important limitation of modified LEFM models is their inability to adequately predict the failure loads of unnotched specimens (or initially uncracked structures), especially those of small size. Though the TPFM satisfactorily predicts the failure loads of large uncracked structures, the SEM cannot be directly applied to these cases (Elices *et al.*,

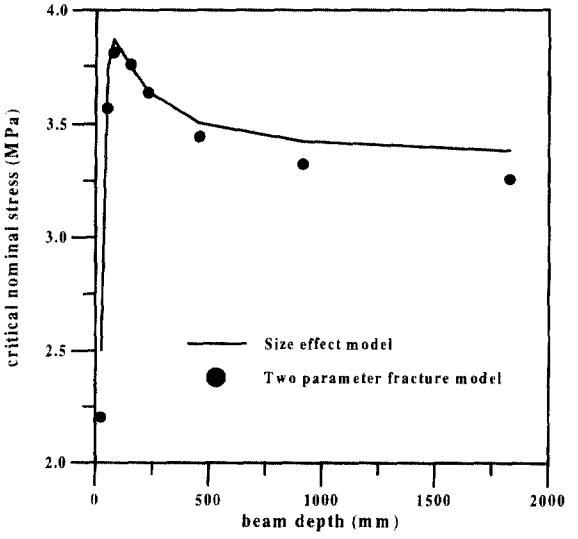

Fig. 2. Comparison of the size effect and two parameter fracture models.

1996). The fundamental reason for this is that the LEFM functions used by the models are not applicable to these cases since K_I and its derivative vanish for a crack length of zero size (Planas and Elices, 1990b).

COMPARISON WITH THE MULTIFRACTAL SCALING MODEL

Considering that the effect of the disorder in the microstructure on structural behaviour becomes progressively less significant as the size of the structure increases, Carpinteri *et al.* (1995) formulated a model called the multifractal scaling law (MFSL) for representing the size effect on the failure loads. Furthermore, they assumed that the effect of the disorder tends to reduce the nominal failure until it reaches a constant value equal to the tensile strength at infinite size. By associating the degree of disorder to a multiple of the aggregate size l_c, which is assumed to be a material parameter, the model is defined as:

$$\sigma_N = f_t \sqrt{1 + \frac{l_c}{d}} \tag{7}$$

Contrary to the SEM and other nonlinear fracture mechanics models, the MFSL assumes that LEFM is applicable at small sizes and crack lengths. Another important difference is that eqn (7) is independent of the geometry of the specimen and the initial crack length.

DETAILS OF THE TESTS PERFORMED IN THE PRESENT STUDY

Two concretes were used in the experimental study. The first one was a conventional concrete, denoted as NSC, with a cement : sand : gravel : water proportion of 1 : 2.05 : 2.05 : 0.5, by weight. Spanish Type I-45 A cement (equivalent to ASTM type I and CEN Class I 42.5 cement), siliceous sand (0–5 mm), and crushed limestone gravel (5–12 mm) were the materials used. The slump of the fresh concrete was 14 cm. The average 28-day values of the conventional compression strength (f_c) and the Brazilian splitting-tensile strength (f_{st}) were 35.9 MPa ($\pm 7.2\%$) and 3.8 MPa ($\pm 14.8\%$), respectively. Both tests were performed on 15×30 cm cylinders.

The second concrete was a high-strength silica fume concrete, denoted as HSC. The cement : sand : gravel : water : microsilica proportions were 1 : 1.9 : 1.9 : 0.35 : 0.1, by weight. The materials used were Spanish I 55-A cement (equivalent to ASTM type III and CEN Class I 52.5 cement), siliceous sand (0–5 mm), crushed limestone gravel (5–12 mm) and densified condensed silica fume (ELKEM Grade 920D). A napthalene-based superplasticizer (GRACE Daracem 120) was incorporated at 17.8 l/m^3 of concrete (dry superplasticizer/cement = 1.5%, by weight). The slump of the fresh concrete was 25 cm. The average 28-day values of the conventional compression strength (f_c) and the Brazilian splitting-tensile strength (f_{st}), from 15×30 cm cylinders, were 81.7 MPa ($\pm 1.5\%$) and 5.3 MPa ($\pm 10.1\%$), respectively.

For the fracture tests, the beams were cast in laminated wooden moulds (with the loading plane vertical), by placing the concrete in three layers, each of which was compacted by rodding. They had depths (d) of 80, 160 and 320 mm, with the same thickness (b) of 50 mm and lengths equal to 3.125 d. In all 56 beams were tested.

The beams were tested under three-point bending (i.e., centre-point loading) with spans (s) equal to 2.5d. The specimens tested, along with their notch lengths (a_0), are specified in Table 1. In some cases (denoted with *), the specimens were cut from the halves of previously-tested larger specimens. The notches were cut in the bottom (moulded) faces with a diamond disc saw, and had widths of 3 mm. All the tests were conducted in a 1MN Instron 8505 dynamic testing system under crack-mouth opening displacement (CMOD) control. The constant CMOD rates used in each test are also given in Table 1; different loading rates were used in order to get similar failure times. The CMOD was monitored using a clip gauge of ± 2 mm range and the load was monitored using a load cell of ± 100 kN range.

Table 1. Test data for the NSC and HSC specimens

Specimen notation	Beam depth (d) mm	Notch length (a_0) mm	CMOD rate microns/s	Peak load N	Peak load corrected for self weight (P_u) N	Maximum nominal stress (σ_N) MPa
(a) NSC						
NS1	320	88	0.10	9369	9557	0.594
				9385	9573	0.595
				9439	9629	0.599
NS2*	160	44	0.07	5650	5697	0.711
				5000	5047	0.629
				4779	4826	0.602
NS3*	80	22	0.03	2751	2763	0.692
				3157	3169	0.792
				2956	2967	0.741
NN1	320	12	0.05	16,950	17,138	1.071
			0.04	17,930	18,118	1.132
NN2	160	12	0.05	8280	8327	1.041
				7560	7607	0.951
				8180	8227	1.028
NN3	80	12	0.03	3990	4002	1.000
			0.02	4280	4292	1.073
ND1	160	0	0.03	11,740	11,787	1.473
				12,660	12,707	1.588
ND2*	160	32	0.07	7530	7557	0.947
				6050	6097	0.762
				5970	6017	0.752
ND3*	160	64	0.05	3480	3527	0.441
				3590	3637	0.455
				3100	3147	0.393
ND4*	160	96	0.03	1770	1817	0.227
				1350	1397	0.175
				1770	1817	0.227
(b) HSC						
HS1	320	88	0.10	9700	9888	0.618
				9740	9928	0.621
				9740	9928	0.621
HS2*	160	44	0.07	5542	5589	0.699
				5365	5412	0.677
				5533	5580	0.698
HS3*	80	22	0.03	3763	3775	0.944
				3345	3357	0.839
				3496	3508	0.877
HN1	320	12	0.05	22,060	22,248	1.391
				21,260	21,448	1.341
				21,180	21,368	1.336
HN2	160	12	0.05	10,330	10,337	1.297
				10,598	10,645	1.331
				10,727	10,774	1.347
HN3	80	12	0.03	5644	5656	1.414
				5216	5228	1.307
				5159	5171	1.293
HD1*	160	0	0.03	20,410	20,457	2.557
				17,720	17,767	2.221
HD2*	160	32	0.07	7147	7194	1.124
				7227	7274	1.137
				6887	6934	1.083
HD3	160	66	0.05	3700	3747	0.781
				4070	4117	0.858
				4290	4337	0.904
HD4*	160	96	0.03	1766	1813	0.567
				1716	1763	0.551
				1776	1823	0.570

* Specimens cut from larger beams.

In order to compensate for the effect of the weight of the specimen on the measured peak load, the corrected peak load (P_u in Table 1) is obtained by adding half the self-weight to the measured load (as in RILEM, 1990). The maximum nominal stress (σ_N) is taken as

P_u/bd. Note that in order to obtain a nominal maximum flexural stress, σ_N has to be multiplied by 1.5 s/d (Bažant and Kazemi, 1990).

DETERMINATION OF THE PARAMETERS OF SEM AND MFSL

The data from the geometrically similar specimens are used to determine the fracture parameters or to calibrate the SEM, for each concrete. Considering two-dimensional similarity, the specimens NS1, NS2 and NS3 of NSC, and specimens HS1, HS2 and HS3 of HSC have scaled dimensions, with a span/depth ratio (s/d) of 2.5 and relative notch length ($\alpha_0 = a_0/d$) of 0.275 d. The corresponding values of $g(\alpha_0)$ and $g'(\alpha_0)$ are 11.23 and 59.71, respectively.

Using eqn (3) the parameters B and d_0 have been determined through nonlinear regression analysis with the Marquardt–Levenberg algorithm. The plot of the fit with the test data is shown in Fig. 3. It can be seen that the trend is modeled satisfactorily, and that the HSC data lie closer to the LEFM asymptote (and have higher β values) than the NSC data, reflecting the higher brittleness of silica fume concretes compared with conventional concretes. The values obtained from the regression analysis and the resulting fracture parameters are given in Table 2. The modulus of elasticity for each concrete was obtained from the initial slope of the load–CMOD curves of the largest notched beams. The trends of the parameters are as expected, with the HSC exhibiting a higher value of B and a lower value of d_0 than NSC, indicating higher strength and higher brittleness, respectively. The higher brittleness is also reflected in the lower c_f and δ_c values of HSC.

The process of determining the fracture parameters with data from proportional specimens can be considered as the calibration of the size effect model. These are material parameters which can be used in the generalized model (eqn 6) to predict the failure loads of other specimens and structures. The only additional requirement is the determination of the LEFM function $g(\alpha)$ for the geometry whose failure load has to be predicted. Moreover, the calibration can be performed on specimens cut from the undamaged parts of previously-tested larger specimens or constructed structures, as in the present study. This eliminates

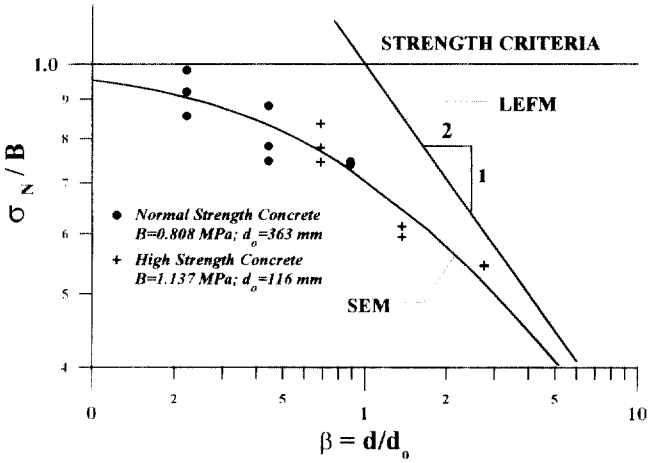

Fig. 3. Calibration of the size effect model for normal (NSC) and high strength (HSC) concretes using geometrically similar specimens.

Table 2. Fracture parameters from the size effect method

Concrete	f_c MPa	f_{sy} MPa	E GPa	B MPa	d_0 mm	K_{Ic} MPa-mm$^{1/2}$	c_f mm	G_f N/m	δ_c microns
NSC	36.4	3.4	34.5	0.806	363	50.7	66	74.5	38.1
HSC	83.0	4.4	36.4	1.137	116	41.2	22	46.6	17.0

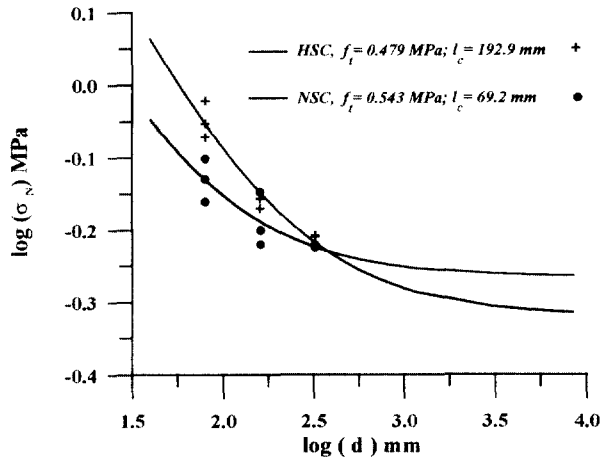

Fig. 4. Fitting of the multifractal scaling model to test data.

the need for several sets of moulds and reduces the quantity of material needed for the tests.

The MSFL has also been fitted to the above-mentioned data (Fig. 4). The fits of the test data are satisfactory and the fracture parameters obtained are: $f_t = 0.543$ MPa and $l_c = 69$ mm for NSC, and $f_t = 0.480$ MPa and $l_c = 193$ mm for HSC. In order to compare the values of f_t obtained from the MFSL to test data, they are converted to the flexural strengths of 2.04 for NSC and 1.8 for HSC, by multiplying them by 1.5 s/d. Note that these values are much lower than the experimental data (see f_{sf} values in Table 2). These data also imply that the theoretical flexural strength decreases with an increase in compressive strength. Similarly, the l_c values, which are measures of the microstructural disorder and consequently the material ductility, indicate an increase in disorder and a decrease in the brittleness with an increase in compressive strength. These trends seem to be contrary to those in the literature (cf Gettu and Shah, 1994).

PREDICTION OF THE SIZE EFFECT IN NON-SIMILAR SPECIMENS

Other than the scaled specimens, two other series of the specimens were tested for each concrete. One series had specimens of the same size ($d = 160$ mm) with notches of different lengths, consisting of the specimens ND1, ND2, ND3, ND4 and NS2 for NSC, and HD1, HD2, HD3, HD4 and HS2 for HSC (see Fig. 5 for typical load–CMOD and load–deflection curves). The other series had specimens of different sizes with the same notch length ($a_0 = 12$ mm), consisting of the specimens NN1, NN2 and NN3 for NSC, and HN1, HN2 and HN3 for HSC.

The predictions made with eqn (6) for the first series are plotted in Fig. 6, along with the experimental data. Note that this series had relative notch lengths (α_0) ranging from zero (i.e., unnotched) to 0.6. It can be seen that the failure load predictions are good, in both concretes, for longer notch lengths. The predictions also reflect the higher rate at which the strength of the HSC specimen decreases with an increase in crack length due to its higher brittleness. However, the model severely underestimates the strength of unnotched specimens ($a_0 \to 0$), with a higher error for the more brittle high strength concrete. Also, it appears that the deviation from the experimental trend occurs at a smaller notch length in the less brittle normal-strength concrete. This indicates that the SEM is not directly applicable for the case of short cracks and initially uncracked specimens, confirming the conclusion of Planas and Elices (1990b). This aspect is also reflected in Fig. 5, where it can be seen that the brittleness number β is able to quantify the brittleness of the failure (indicated by the steepness of the descending part of the curves) only for values of $\alpha_0 > 0.2$. It appears that these cases have to be simulated through more sophisticated procedures such as the

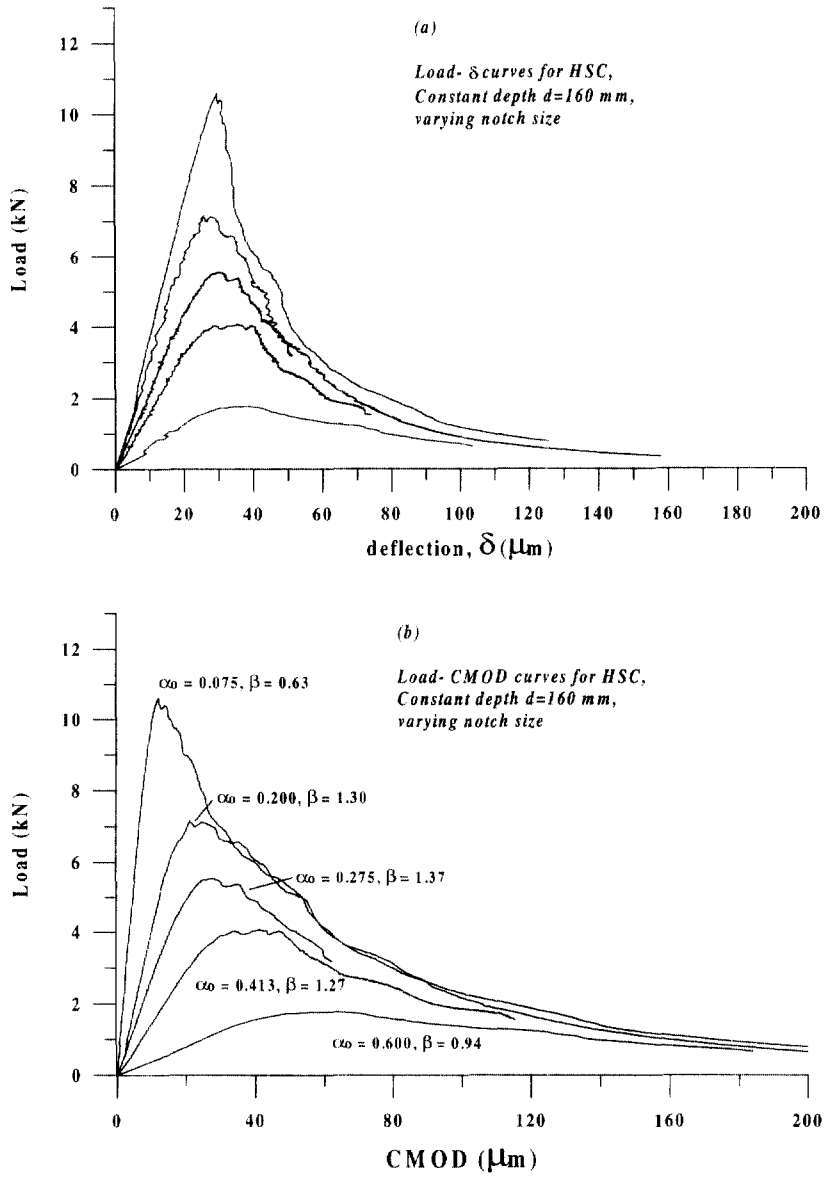

Fig. 5. Test data corresponding to high strength concrete beams of constant size and different notch lengths—(a) Load–deflection curves, (b) Load–CMOD curves.

analysis with the fictitious crack model as suggested by Elices *et al.* (1996) or through the coupling of damage and fracture criteria as suggested by Mazars and Pijaudier-Cabot (1994), and Bažant and Li (1995).

The predictions and test data corresponding to the second series of specimens are shown in Fig. 7. The geometrically similar specimens have depths of 80, 160 and 320 mm (i.e., scale of 1 : 4) with a constant notch length of 12 mm, which is small compared to the depth and the aggregate size. It can be seen that the predictions are close to the test data. However, the range of the data is insufficient to completely verify the trends exhibited by the model predictions.

The multifractal model could not be used to predict the loads in these specimens since this model does not incorporate the notch length. On the other hand, fitting of the data with the model yielded negative values of l_c, which seem unrealistic. The physical significance of the MFSL parameters and their applicability have therefore to be studied further and clarified.

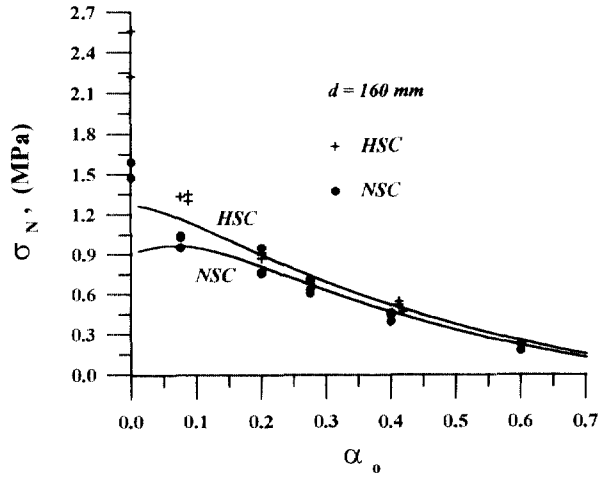

Fig. 6. Predictions of the size effect model and the experimental data for specimens of constant size (d = 160 mm) and different notch lengths.

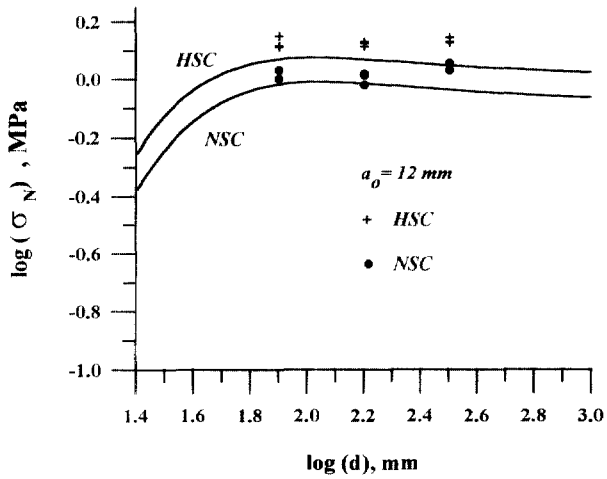

Fig. 7. Predictions of the size effect model and the experimental data for specimens of varying size (d = 80, 160, 320 mm) and constant notch length (a_0 = 12 mm).

CONCLUSIONS

The size model effect of Bažant provides a framework for the characterization of the fracture behaviour of concrete and for the determination of the parameters that quantify the crack resistance and the material brittleness. Comparisons with the multifractal model indicate that though the fits of the data from geometrically similar specimens are satisfactory for both the models, the SEM provides much more meaningful parameters and is capable of predicting the strengths of concrete specimens and structures. Using the parameters determined from simple notched beam tests, the SEM can predict the failure loads of other structures. The predictions are practically exact when the initial crack length is not small compared to the aggregate size and the specimen dimensions. For small notches and initial cracks, the model underestimates the failure loads.

Acknowledgements—Partial financial support from Spanish DGICYT grants PB93-0955, MAT93-0293 and MAT96-0967 to the UPC is acknowledged. H. Saldivar is supported by fellowships from MUTIS (Spain) and CONACYT (México) during his doctoral study at the UPC. R. Gettu gratefully appreciates several stimulating discussions with Profs V. S. Gopalaratnam and A. Aguado on the topic. This paper corresponds to the presentation made at the SES Prager Symposium (Phoenix, U.S.A., 1996) in honour of Prof. Z. P. Bažant.

REFERENCES

Bažant, Z. P. (1984) Size effect in blunt fracture: concrete, rock, metal, *J. Engng Mech.* **110**(4), 289–307.

Bažant, Z. P. and Pfeiffer, P. A. (1987) Determination of fracture energy from size effect and brittleness number. *ACI Mater. J.* **84**(6), 463–480.

Bažant, Z. P. and Kazemi, M. T. (1990) Determination of fracture energy, process zone length and brittleness number from size effect, with application to rock and concrete. *Int. J. Fracture* **44**, 111–131.

Bažant, Z. P., Gettu, R. and Kazemi, M. T. (1991) Identification of nonlinear fracture properties from size effect tests and structural analysis based on geometry-dependent R-curves. *Int. J. Rock Mech. Min. Sci.* **28**(1), 43–51; Corrigenda; **28**(2/3), 233.

Bažant, Z. P., Ozbolt, J. and Eligehausen, R. (1994) Fracture size effect: Review of evidence for concrete structures. *J. Struct. Engng* **120**(8), 2377–2398.

Bažant, Z. P. and Li, Z. (1995) Modulus of rupture: size effect due to fracture initiation in boundary layer. *J. Struct. Engng* **121**(4), 739–746.

Carpinteri, A., Chiaia, B. and Ferro, G. (1995) Size effects on nominal tensile strength of concrete structures: multifractality of material ligaments and dimensional transition from order to disorder. *Mater. Struct.* **28**, 311–317.

Elices, M. and Planas, J. (1991) Size effect and experimental validation of fracture models. In *Analysis of Concrete Structures by Fracture Mechanics*, ed. L. Elfgren and S. P. Shah, pp. 99–127. Chapman and Hall, London, U.K.

Elices, M. and Planas, J. (1993) The equivalent elastic crack: I. Load-Y equivalences. *Int. J. Fracture*, **61**, 259–272.

Elices, M., Guinea, G. V. and Planas, J. (1996) Prediction of size-effect based on cohesive crack models. In *Size-Scale Effects in the Failure Mechanisms of Materials and Structures*, ed. A. Carpinteri, pp. 309–324. E&FN Spon, London, U.K.

Gettu, R. and Shah, S. P. (1994) Fracture mechanics. In *High Performance Concretes and Applications*, ed. S. P. Shah and S. H. Ahmad, pp. 161–212. Edward Arnold, London, U.K.

Gettu, R., Ariño, A. and Kazemi, M. T. (1995) Discussion of Fracture mechanics and size effect of concrete in tension. *J. Struct. Engng* **121**(1), 151–153.

Hillerborg, A. (1983) Analysis of one single crack. In *Fracture Mechanics of Concrete*, ed. F. H. Wittmann, pp. 223–250. Elsevier Applied Science, Amsterdam, The Netherlands.

Jenq, Y. S. and Shah, S. P. (1985) A two parameter fracture model for concrete. *J. Engng Mech.* **111**, 1227–1241.

Karihaloo, B. L. (1995) *Fracture Mechanics and Structural Concrete*. Longman Scientific and Technical, Harlow, U.K.

Mazars, J. and Pijaudier-Cabot, G. (1994) Damage localization analysed as a crack propagation. In *Fracture and Damage in Quasibrittle Structures*, ed. Z. P. Bažant, Z. Bittnar, M. Jirásek and J. Mazars, pp. 145–157. E&FN Spon, London, U.K.

Mihashi, H., Nomura, N. and Kim, J. K. (1996) Fracture mechanics properties and size effect in concrete. *Size-Scale Effects in the Failure Mechanisms of Materials and Structures*, ed. A. Carpinteri, pp. 399–410. E&FN Spon, London, U.K.

Planas, J. and Elices, M. (1990a) Fracture criteria for concrete: mathematical approximations and experimental validation. *Engng Fract. Mech.* **35**(13), 87–94.

Planas, J. and Elices, M. (1990b) Anomalous structural size effect in cohesive materials like concrete. *Serviceability and Durability of Construction Materials*, ed. B. A. Suprenant, pp. 1345–1356. American Society of Civil Engineers, New York, USA.

RILEM (1990) Size-effect method for determining fracture energy and process zone size of concrete. Draft Recommendation FMC2, Committee TC89-FMT. *Mater. Struct.* **23**(3), 461–465.

Tang, T., Shah, S. P. and Ouyang, C. (1992) Fracture mechanics and size effect of concrete in tension. *J. Struct. Engng* **18**(11), 3169–3185.